Tendon and Motor Phenotypes in the *Crtap*$^{-/-}$ Mouse Model of Recessive Osteogenesis Imperfecta

Matthew W. Grol[1], Nele A. Haelterman[1], Elda M. Munivez[1], Marilyn Archer[2], David Hudson[2], Sara F. Tufa[3], Douglas R. Keene[3], David Eyre[2] and Brendan H. Lee[1†]

[1] Department of Molecular and Human Genetics, Baylor College of Medicine, Houston, TX

[2] Department of Orthopaedics and Sports Medicine, University of Washington, Seattle, WA

[3] Shriners Hospital for Children, Portland, OR

[†] Correspondence and reprint requests:

Brendan H. Lee, MD, PhD

Department of Human and Molecular Genetics

One Baylor Plaza, ABBR-R814

Baylor College of Medicine

Houston, TX 77030

Email: blee@bcm.edu

Tel: +1 713-798-7246

Fax: +1 713-798-4523

Running Title: Tendon and motor deficits in Osteogenesis Imperfecta

Keywords: osteogenesis imperfecta, tendon, ligament, cross-link, motor behavior

ABSTRACT

Osteogenesis imperfecta (OI) is a heterogeneous group of connective tissue disorders characterized by variable short stature, skeletal deformities, low bone mass with increased bone fragility, and motor deficits. The majority of cases are caused by mutations in type I collagen, or by mutations that affect collagen processing and/or modification. Like bone, the extracellular matrix of tendons and ligaments is largely made up of type I collagen; however, despite the fact that a subset of OI patients presents with joint hypermobility, how tendon/ligament dysfunction contributes to this is unknown. Here, we performed a detailed phenotypic characterization of the flexor digitorum longus (FDL) tendon, Achilles tendon and patellar ligament in the *Crtap* mutant mouse model of severe, recessive OI. Stable, pyridinoline collagen cross-links were increased by 5- to 10-fold in mutant tendons and ligaments. Collagen fibril size in all three structures was also smaller in *Crtap*$^{-/-}$ mice compared to wildtype or heterozygous littermates. Together, these ultrastructural and biochemical changes resulted in thinner tendons and ligaments with increased cellularity compared to controls, as assessed by histology. To examine how alterations in tendons might affect motor function, we performed a battery of behavioral assays. During open field assessment, *Crtap*$^{-/-}$ mice exhibited reduced horizontal and vertical activity. *Crtap*$^{-/-}$ mice also exhibited motor impairments on the rotarod and grid footslip tests. In addition, *Crtap*$^{-/-}$ mice had reduced grip strength and displayed reduced time on the inverted grid test, indicating that they are weaker than wildtype and heterozygous mice. In summary, these data demonstrate that the tendons/ligaments of *Crtap*$^{-/-}$ mice are pathologically altered compared to wildtype – a phenotype that correlates with motor deficits and grip strength impairments. As such, *Crtap*$^{-/-}$ mice provide a preclinical model with which to examine downstream mechanisms and therapies pertaining to tendon/ligament pathology and motor dysfunction for OI patients.

INTRODUCTION

Tendon is a fibrous tissue that connects skeletal muscle to bone to facilitate motion, whereas ligaments connect articulating bones to support joint alignment and function[1, 2]. The extracellular matrix of tendons and ligaments is primarily composed of type I collagen as well as smaller quantities of other collagens and proteoglycans[3]. During development, the collagen fibrils in tendons and ligaments develop through addition and lengthening before transitioning to appositional fusion of existing fibers with continued lengthening in post-natal life[4]. The synthesis and assembly of this collagen-rich matrix is influenced by other small collagens and proteoglycans as well as by the cross-linking chemistry of type I procollagen fibrils, which in turn regulates fibril size and strength[5]. Like tendon and ligament, the organic matrix of bone consists largely of type I collagen[6], and disruptions in collagen synthesis and folding have been shown to negatively impact its biochemical and mechanical properties in connective tissue diseases such as Osteogenesis Imperfecta (OI)[7]. However, despite evidence of joint mobility phenotypes and motor deficits in OI patients[8, 9], tendon and ligament phenotypes in this disease are relatively understudied.

OI is a heterogeneous group of disorders characterized by variable short stature, skeletal deformities, low bone mass, and increased bone fragility. Approximately 80% of OI cases are caused by dominantly inherited mutations in the genes encoding the α1(I) or α2(I) chains of type I collagen. Mutations in genes responsible for the synthesis, post-translational modification and processing of collagen, such as cartilage-associated protein (CRTAP), lead to severe, recessive forms of this disease[7]. In addition to skeletal defects, other connective tissue manifestations including joint hypermobility and skin hyperlaxity are observed in a subset of OI patients[8, 9]. Our and others' studies have shown that CRTAP forms a complex with Prolyl 3-

hydroxylase 1 (P3h1, encoded by *Lepre1*) and Cyclophilin B (CypB, encoded by *Ppib*), and is required for prolyl 3-hydroxylation of type I procollagen at Pro986 of chain α1(I) and Pro707 of chain α2(I)[10-12]. In this regard, loss of either CRTAP or P3H1 leads to loss of this complex and its activity, causing a severe recessive form of OI characterized by short stature and brittle bones[11, 13-15]. Collagen isolated from *Crtap*$^{-/-}$ and *Lepre1*$^{-/-}$ mice is characterized by lysine over-modifications and abnormal fibril diameter[11, 14]. A comprehensive analysis of *Crtap*$^{-/-}$ mice has revealed multiple connective tissue abnormalities, including in lungs, kidneys, and skin[16]; however, the impact of loss of Crtap on tendons and ligaments remains unknown.

Alterations in collagen fibril size and cross-linking have been noted in a limited number of studies using dominant or recessive mouse models of OI[17-19]; however, whether loss of Crtap impacts tendon and ligament development and structure remains unknown. In this study, we show that *Crtap*$^{-/-}$ mice have thinner Achilles tendons and patellar ligaments at 1 and 4 months-of-age that are hypercellular with a reduction in total ligament volume. Moreover, the patellar and cruciate ligaments from *Crtap*$^{-/-}$ show increased cell size and variable ectopic chondrogenesis by 4 months-of-age. Examining the collagen matrix, we found an increase in stable (irreversible) collagen cross-links at both timepoints, accompanied by alterations in fibril diameter at 4-months compared to wildtype controls. These changes in the tendons and ligaments of *Crtap*$^{-/-}$ mice were accompanied by motor deficits and reduced strength at 4 months-of-age. In conclusion, loss of Crtap in mice causes a tendinopathy-like phenotype and significant behavioral impairments.

MATERIALS AND METHODS

Animals

Crtap$^{-/-}$ mice were generated as previously described[11] and maintained on a mixed C57BL/6J and 129Sv genetic background. All studies were performed with approval from the Institutional Animal Care and Use Committee (IACUC) at Baylor College of Medicine. Mice were housed 3 to 4 mice to a cage in a pathogen-free environment with *ad libitum* access to food and water and under a 14h light/10h dark cycle.

Histological analysis

Mice were euthanized and ankle and knee joints were dissected and fixed for 48 h on a shaker at room temperature in freshly prepared 4% paraformaldehyde (PFA) in 1× phosphate-buffered saline (PBS). Samples were decalcified at 4°C using 10% ethylenediaminetetraacetic acid (EDTA) in 1×PBS for 10 days (with one change out at 5 days) prior to paraffin embedding using a standard protocol. Samples were sectioned at 6 μm and stained with hematoxylin and eosin (H&E) to visualize tendon structures.

Phase-contrast μCT imaging and analysis

To quantify tendon/ligament volume, knee joints were dissected from mice, stained with contrast agents, scanned by phase-contrast μCT, and analyzed using TriBON software (RATOC, Tokyo, Japan) as previously described for articular cartilage[20-23]. In addition to the articular surfaces (data not shown), we performed contrast-enhanced visualization of the patellar ligament using this protocol. To quantify volume, samples were examined in transverse where the patellar ligament boundary was easily distinguished from the joint capsule. Ligament volume was assessed from its origin within the patella to its insertion at the tibia.

Transmission electron microscopy analysis of collagen fibril size

Mouse ankle and knee joints were dissected and fixed in fresh 1.5% glutaraldehyde/1.5% PFA (Tousimis) with 0.05% tannic acid (Sigma) in 1×PBS at 4°C overnight to preserve the native tension on relevant tendons/ligaments. The next day, flexor digitorum longus (FDL) and Achilles tendons as well as patellar ligament were dissected out in 1×PBS, and placed back into fixative. Samples were then post-fixed in 1% osmium tetroxide (OsO_4), rinsed in Dulbecco's Modified Eagle Medium (DMEM) and dehydrated in a graded series of ethanol to 100%. Samples were rinsed in propylene oxide, infiltrated in Spurrs epoxy, and polymerized at 70°C overnight. TEM images were acquired using a FEI G20 TEM at multiple magnifications to visualize transverse sections of collagen fibrils. Collagen fibril diameter was measured using the Fiji release of ImageJ[24].

Tendon collagen cross-linking analysis

Collagen hydroxylysyl-pyridinoline (HP) cross-links were quantified as previously described[25, 26]. In brief, tendons and ligaments isolated from hindlimbs were hydrolyzed by 6M HCl for 24h at 108°C. Dried samples were then dissolved in 1% (v/v) n-heptafluorobutyric acid for quantitation of HP by reverse-phase HPLC with fluorescence monitoring.

Open field assessment of spontaneous motor activity

Open field activity was measured using the VersaMax Animal Activity Monitoring System (AccuScan Instruments, Columbus, OH). On the day of assessment, mice were transferred to the test room and allowed to acclimate in their home cage for 30 min at 50 Lux of illumination with 60 dB of white noise. Mice were then placed individually into clear 40 cm × 40 cm × 30 cm

chambers and allowed to move freely for 30 min. Locomotion parameters and zones were recorded using the VersaMax activity monitoring software. Chambers were cleaned with 30-50% ethanol to remove the scent of previously tested mice between each run.

Rotarod analysis of motor coordination and endurance

On the day of assessment, mice were transferred to the test room and allowed to acclimate within their home cage for 30 min at 50 Lux of illumination with 60 dB of white noise. Mice were then placed on a rotarod (UGO Basile, Varese, Italy) set to accelerate from 5-to-40 RPM over 5 min. Five trials were performed per day for 2 consecutive days (trials 1-10) with a rest time of 5 min between trials. Latency to fall was recorded when the mouse fell from the rotating rod or went for two revolutions without regaining control. The rotarod was cleaned with 30-50% ethanol between mice to remove the scent of previously tested animals.

Grid footslip analysis of motor coordination

The grid footslip assay consisted of a wire grid set atop a stand where movement was recorded by a suspended digital camera. Mice were transferred to the test room on the day of assessment, and allowed to acclimate within their home cage for 30 min at 50 Lux of illumination with 60 dB of white noise. Mice were then placed one at a time on the grid and allowed to move freely for 5 min. The observer sat 6-8 feet away at eye-level to the mouse and recorded forelimb and hindlimb footslips using the ANY-maze video tracking software (Stoelting Co., Wood Dale, IL). At the completion of the test, mice were removed to their original home cage. Forelimb and hindlimb footslips were normalized to the total distance traveled during the test.

Inverted grid analysis of strength and endurance

On the day of assessment, mice were transferred to the test room and allowed to acclimate within their home cage for 30 min at 50 Lux of illumination with 60 dB of white noise. Mice were then placed in the middle of a wire grid, held approximately 18-in above a cushioned pad and inverted. The latency to fall for each mouse was recorded. At the completion, mice were returned to their home cage.

Grip strength analysis

Mice were transferred to the test room on the day of assessment, and allowed to acclimate within their home cage for 30 min at 50 Lux of illumination with 60 dB of white noise. Each mouse was then lifted by its tail onto the bar of a digital grip strength meter (Columbus Instruments, Columbus, OH). Once both forepaws had gripped the bar, the mouse was pulled away from the meter by its tail with a constant speed until the forepaws released. The grip (in N of force) was recorded and the procedure repeated twice for a total of three measurements, which were averaged for the final result.

Statistical analysis

Data are presented as means ± S.D. or min-to-max box and whisker plots with individual data points. In the case of normal distribution, groups were compared using one-way ANOVA followed by Tukey's post-hoc tests. For non-normal distribution, groups were compared using Kruskal-Wallis followed by Dunn's post-hoc tests. For the Rotarod assay where time was a variable, groups were compared using two-way ANOVA followed by Bonferroni's post-hoc tests. Statistical analysis was performed using Prism 8.3.1 (GraphPad Software, La Jolla, CA).

185 For all tests, a *p*-value of < 0.05 was considered statistically significant.

186

187 **RESULTS**

188 *Crtap*$^{-/-}$ *mice exhibit abnormal tendon development*

189 Mice lacking Crtap present with growth delay, rhizomelia, and severe osteoporosis together with
190 disruption of other connective tissues including lung and skin[11, 16]. To assess whether *Crtap*$^{-/-}$
191 mice exhibit disruptions in the development of tendons and ligaments, we harvested ankle and
192 knee joints at 1 and 4 months-of-age to histologically examine the Achilles tendon and patellar
193 ligament. At 1-month, *Crtap*$^{-/-}$ mice presented with thinner Achilles tendons and patellar
194 ligaments (**Figure 1C,F**) with increased cell numbers in both structures compared to wildtype
195 (**Figure 1A,D**) and heterozygous mice (**Figure 1B,E**). There was also a prominent hyperplasia of
196 the synovial membrane in *Crtap* mutant knees at this age (**Figure 1F**). By 4 months-of-age,
197 *Crtap*$^{-/-}$ Achilles tendons and patellar ligaments remained thinner and hypercellular compared to
198 wildtype and heterozygous mice (**Figure 1G-L**); in addition, synovial hyperplasia persisted
199 within *Crtap*$^{-/-}$ knees (**Figure 1L**). Interestingly, ectopic chondrogenesis was present towards
200 either end of the patellar ligament and/or cruciate ligaments in some (but not all) 4-month-old
201 *Crtap*$^{-/-}$ mice (**Figure 1L**) – a phenomenon that can occur in tendinopathy[27].

202 To more accurately quantify the differences in tendon/ligament size between genotypes,
203 we employed phase-contrast μCT to examine differences in patellar ligament volume between
204 genotypes (**Figure 1M,N**) – a technique we previously used to examine soft tissues including
205 articular cartilage in intact murine knee joints[20-23]. In 4-month-old mice, we observed a thinning
206 of the patellar ligament compared to wildtype mice, with no notable changes in articular cartilage
207 surface (**Figure 1M**). Quantification revealed a decrease in patellar ligament volume in *Crtap*$^{-/-}$

but not heterozygous mice compared to wildtype controls (**Figure 1N**). Taken together, these histological and μCT data demonstrate that *Crtap*$^{-/-}$ mice display disruptions in the development and postnatal maturation of tendons and ligaments.

Collagen fibril formation is altered in heterozygous and Crtap$^{-/-}$ *mice*

Tendons develop embryonically via increased fibril length and number, whereas postnatal growth arises from an increase in fibril length and diameter – the latter of which is driven by lateral fusion of smaller fibrils[4]. To investigate the role of Crtap in collagen fibril maturation, we utilized transmission electron microscopy (TEM) to examine changes in fibril diameter in flexor digitorum longus (FDL) and Achilles tendons as well as patellar ligaments (**Figure 2**). In the FDL tendon, there was a marked increase in small collagen fibrils (20-60 nm in size), a reduction in 80-320 nm fibrils, and a slight increase in larger fibrils (>340 nm in diameter) in *Crtap*$^{-/-}$ mice compared to wildtype (**Figure 2A,C,D**). Despite similarities seen in histology, heterozygous mutant FDL tendons also exhibited a slight increase in 20-40 nm fibrils in mice compared to wildtype controls (**Figure 2A-B,D**). Similar trends were observed for the Achilles tendon, namely an increase in small fibrils (20-60 nm), a reduction in 80-240 nm fibrils and an increase in large fibrils (> 280 nm) upon loss of *Crtap* (**Figure 2E,G-H**). In contrast to what we observed for the FDL, heterozygous *Crtap*$^{-/+}$ Achilles tendons did not have increased numbers of smaller fibers (**Figure 2F,H**). Instead, a greater number of fibrils ranging from 140-200 nm in size was noted compared to wildtype controls.

Compared to the FDL and Achilles tendons, the greatest differences were seen within the patellar ligament, though the pattern of changes remained consistent (**Figure 2I-L**). Specifically, we observed a dramatic increase in 20 nm collagen fibrils compared to both heterozygous and

wildtype mice (**Figure 2I-L**). Fibrils ranging from 100-180 nm in diameter were reduced in heterozygous and *Crtap*$^{-/-}$ mice compared to wildtype. Interestingly, the greatest difference from wildtype was an increase in large collagen fibrils (>200 nm) in both heterozygous and *Crtap*$^{-/-}$ mice (**Figure 2I-L**). Taken together, these data indicate that heterozygosity and complete loss of Crtap alters collagen fibril assembly in tendons and ligaments. In addition, the degree to which collagen assembly is affected is site-dependent.

Collagen cross-linking is increased in heterozygous and Crtap$^{-/-}$ *mice*

Along with P3H1 and CyPB, CRTAP is an integral part of the collagen prolyl 3-hydroxylation complex that is responsible for 3-hydroxylation of Pro986 of the type I procollagen α1 chain[7]. Loss of this complex blocks 3-hydroxyproline formation and affects lysine hydroxylation and cross-linking in bone collagen[11, 12]; however, whether *Crtap*$^{-/-}$ mice exhibit altered collagen cross-linking in tendon is unknown. To investigate this, we harvested tendons and ligaments at 1- and 4-months and assessed for collagen cross-linking by quantifying the levels of hydroxylysyl-pyridinoline (HP) (**Figure 3**). Overall, we observed an increase in these stable, mature collagen cross-links from 1 to 4 months-of-age in all genotypes for the FDL and Achilles tendons (**Figure 3A-B**). In contrast, for the patellar ligament, age-dependent increases in collagen cross-links were only observed in *Crtap*$^{-/-}$ mice (**Figure 3C**). For FDL tendons, *Crtap*$^{-/-}$ mice had more of these collagen cross-links at 1- and 4-months compared to heterozygous and wildtype mice; however, the content of HP residues per collagen decreased with age in this tissue (**Figure 3A**). Interestingly, in Achilles tendons, an increase in collagen cross-linking was observed in both heterozygous and *Crtap*$^{-/-}$ mice at 1-month compared to wildtype. In contrast, at 4-months, only *Crtap*$^{-/-}$ mice had elevated collagen cross-links, and these levels were greater than those observed

at the earlier timepoint (**Figure 3B**).

Of the tissues examined, the patellar ligament showed the greatest increase in collagen cross-links both with time and across genotypes. Specifically, collagen cross-links were elevated by 5- to 10-fold in *Crtap*$^{-/-}$ patellar ligaments compared to heterozygous and wildtype at 1- and 4-months, respectively (**Figure 3C**). Taken together, these data suggest that *Crtap* is required for proper hydroxylation and cross-linking of collagen fibrils in tendons and ligaments in a semi-dominant fashion, as heterozygous mutant tendons/ligaments display a phenotype that is milder than the phenotype observed for homozygous mutant mice. Importantly, the chemical quality of collagen cross-linking appears to be spatiotemporally regulated and this regulation is differentially affected by loss of a single or both copies of *Crtap*.

Loss of CRTAP leads to deficiencies in motor activity, coordination and strength

To investigate whether the tendon phenotypes observed in *Crtap*$^{-/-}$ have functional consequences, we performed a series of behavioral assays at 4 months-of-age. Using the open field assay to quantify changes in spontaneous motor activity, we observed that *Crtap*$^{-/-}$ mice displayed significant reductions in both horizontal and vertical activity compared to heterozygous and wildtype mice (**Figure 4A-B**). We next examined changes in motor coordination and endurance using the rotarod assay. While no genotype-dependent differences were observed during the learning phase of the assessment (Trials 1-5), *Crtap*$^{-/-}$ displayed a reduction in latency to fall for Trials 6, 9-10 compared to wildtype and Trials 6, 8-10 compared to heterozygous mice (**Figure 4C**). To confirm this observation, we evaluated the mice using the grid footslip assay – an alternative metric for motor coordination. In this regard, we found that *Crtap*$^{-/-}$ mice exhibited a modest increase in forelimb and hindlimb footslips compared to heterozygous and wildtype mice

(**Figure 4D-E**). Taken together, these findings indicate that *Crtap*$^{-/-}$ mice have deficiencies in motor activity and coordination compared to controls.

We next evaluated strength in the *Crtap*$^{-/-}$ mice using the inverted grid and grip strength assays. Interestingly, we observed a decrease in the latency to fall during the inverted grid assay for *Crtap*$^{-/-}$ mice compared to heterozygous and wildtype controls (**Figure 4F**). Using a more quantitative metric, we examined these mice using the grip strength test and found that while wildtype and heterozygous mice could generate approximately 1.3 N of force, mice lacking CRTAP were weaker with a mean grip strength of 0.62 N (**Figure 4G**). Thus, *Crtap*$^{-/-}$ mice display significant reductions in strength together with perturbations in motor activity and coordination – behavioral changes that could be related in-part to their tendon phenotype.

DISCUSSION

In this study, we examined the histological, ultrastructural and biochemical characteristics of tendons and ligaments in the *Crtap*$^{-/-}$ mouse model of severe, recessive OI. We demonstrate that at 1- and 4 months-of-age, *Crtap*$^{-/-}$ have thinner, more cellular Achilles tendons and patellar ligaments compared to heterozygous and wildtype mice. Using phase-contrast μCT imaging, we confirmed that *Crtap*$^{-/-}$ patellar ligaments at 4-months are smaller than those from heterozygous and wildtype mice. Examining collagen fibril organization, we found a marked alteration in small and large fibrils in both heterozygous and *Crtap*$^{-/-}$ mice compared to wildtype that varied in severity depending on the tendon or ligament being examined. Stable, HP cross-links were also elevated at 1- and 4-months in *Crtap*$^{-/-}$ mice compared to wildtype, which indicates an increase in telopeptide lysine hydroxylation and resulting irreversible intermolecular cross-links (see below). Finally, we demonstrate that *Crtap*$^{-/-}$ mice exhibit motor impairments concomitant with

reductions in grip strength – a phenomenon that may be related to the tendon pathology observed in these mice.

While collagen ultrastructure and cross-linking has been documented in mouse models of dominant and recessive OI, there has been only modest histological characterization of tendons and ligaments in these models. In this regard, we demonstrate that *Crtap*$^{-/-}$ mice have thinner Achilles tendons and patellar ligaments at 1- and 4-months. Despite the reduction in size and extracellular matrix, tendons and ligaments from these mice are hypercellular compared to wildtype and heterozygous animals. While the alterations in tendon and ligament size and cellularity may be a result of alterations in the collagen extracellular matrix, it could also be associated with alterations in cellular signaling. In this regard, transforming growth factor beta (TGF-β) signaling is upregulated in bones from *Crtap*$^{-/-}$ mice[28], and elevated TGF-β signaling has been noted in mouse models with increased tendon cellularity and alterations in collagen fibril distribution[29]. Further research is needed to elucidate the mechanisms that contribute to the histological features noted within both tendons and ligaments in these mice.

Collagen fibril assembly is a dynamic process that begins with the formation of many small fibrils that grow longitudinally during development, followed by appositional fusion and continued longitudinal growth as tendons mature[4]. In the present study, we found an increased proportion of small and large collagen fibrils in the FDL and Achilles tendons as well as patellar ligaments of *Crtap*$^{-/-}$ mice compared to wildtype. These distributions varied in severity across the three tissues, with the greatest differences being observed in the patellar ligament. *Lepre1*$^{-/-}$ mice have been reported to display an increased proportion of small collagen fibrils in tail tendons[19], indicating that loss of the 3-prolyl hydroxylase complex alters collagen fibrillogenesis. At the same time, the increased number of small fibers was more pronounced in *Lepre1*$^{-/-}$ mice, and

there was no evidence of an increased proportion of large fibers[19] as observed for *Crtap*$^{-/-}$ mice in this study. Similar to the *Lepre1*$^{-/-}$ mouse model, mice lacking CypB also exhibit a pronounced increase in small collagen fibrils alone within tail tendons[18]. Together, this suggests that despite forming a complex with P3h1 and CypB, loss of Crtap has distinct consequences on collagen fibrillogenesis. In this regard, it is important to note that tail tendons were used for collagen fibril distribution assessments in both *Lepre1*$^{-/-}$ and *Ppib*$^{-/-}$ mice[18, 19], whereas appendicular tendons and ligaments were examined in our study. The difference in tissue type examined might also explain why we observed unique alterations in collagen fibril distribution in heterozygous *Crtap* mice, whereas *CypB* heterozygous tendons were indistinguishable from wildtype[18].

Type I procollagen molecules undergo post-translational modifications within the endoplasmic reticulum, including lysyl-hydroxylation and prolyl-hydroxylation, that are critical for proper collagen synthesis, transport and stability. Specifically, telopeptide lysine hydroxylation results in mature lysyl-pyridinoline (LP) or hydroxylysyl-pyridinoline (HP) residues after lysyl oxidase oxidation, which as permanent, irreversible crosslinks play a role in regulating fibril growth and strength[25, 30]. Previous literature has demonstrated that loss of the 3-prolyl hydroxylase complex caused by deletion of P3h1 (*Lepre1*$^{-/-}$) or Crtap (*Crtap*$^{-/-}$) prevents prolyl 3-hydroxylation of clade A (type I, II and III) collagens and can lead to changes in lysine post-translational modifications due to loss of its chaperone function[10, 11]. In this study, we found that the mature collagen cross-links (HP residues per collagen) were markedly increased in the FDL and Achilles tendons as well as the patellar ligament of *Crtap*$^{-/-}$ mice relative to wildtype. Interestingly, we observed increased cross-links in the Achilles, but not FDL or patellar tendons of 1-month old heterozygous mice, indicating a mild haploinsufficient effect of Crtap on this tendon biochemical property. Outside of the genotype-specific effects, we saw an age-dependent

346 increase in HP residues per collagen in all genotypes. This observation is consistent with a study
347 by Taga and colleagues that reported an increase in 3-hydroxyproline residues in rat tendon
348 collagen (but not bone or skin) that plateaued at 3 months-of-age[31]. Taken together, these data
349 together with the TEM analyses suggest that altered collagen cross-linking in tendons and
350 ligaments from *Crtap*$^{-/-}$ mice may adversely affect collagen fibril assembly.

351 In addition to skeletal deformities and frequent fractures, severe OI is associated with
352 motor impairments including gait abnormalities, chronic pain and reduced muscle strength[8, 9, 32].
353 In this study, we showed that *Crtap*$^{-/-}$ mice exhibit reduced motor activity and coordination using
354 the open field, rotarod and grid footslip assays. We also observed a reduction in latency to fall on
355 the inverted grid assay that was mirrored by a dramatic loss of grip strength compared to
356 heterozygous and wildtype mice. These results are consistent with findings reported for the
357 *Col1a1*$^{Jrt/+}$ mouse model of severe OI and Ehlers-Danlos syndrome[17]. Specifically, Abdelaziz
358 and colleagues found that *Col1a1*$^{Jrt/+}$ mice displayed reduced motor activity using the open field
359 and running wheel assays – a phenotype they attributed to thermal hyperalgesia and mechanical
360 allodynia in these mice[33]. In this regard, the reduced vertical activity we observed in *Crtap*$^{-/-}$
361 mice may be indicative of a pain or spinal phenotype, suggesting that characterization of pain in
362 this model is a useful avenue for future research. Overall, this study represents one of the first
363 extensive characterizations of behavioral deficits in a mouse model of severe, recessive OI that
364 also correlates these deficits to tendon phenotypes.

365 Taken together, this study provides the first evidence for tendon and ligament phenotypes
366 in the *Crtap*$^{-/-}$ mouse model of severe recessive OI. We also provide compelling evidence for a
367 strong motor activity and coordination phenotype in these mice. As quality of life is so impacted
368 in patients with OI, a more comprehensive evaluation of behavioral outcomes in future

preclinical studies may provide important insights into the efficacy of therapeutic interventions.

AUTHOR CONTRIBUTIONS

M. W. Grol: Conception and design of the study, acquisition, analysis and interpretation of data, drafting and editing of manuscript

N. A. Haelterman: Acquisition and analysis of data, editing of manuscript

E. Munivez: Acquisition of data

M. Archer: Acquisition and analysis of data

D. Hudson: Acquisition, analysis and interpretation of data, editing of manuscript

S. F. Tufa: Acquisition and analysis of data

D. R. Keene: Acquisition, analysis and interpretation of data, editing of manuscript

D. Eyre: Analysis and interpretation of data, editing of manuscript

B H. Lee: Conception and design of the study, interpretation of data, editing of manuscript

Conflicts

No conflicts of interest to report.

Funding

BCM Intellectual and Developmental Disabilities Research Center (HD024064) from the Eunice Kennedy Shriver National Institute Of Child Health & Human Development, the BCM Advanced Technology Cores with funding from the NIH (AI036211, CA125123, and RR024574), the Rolanette and Berdon Lawrence Bone Disease Program of Texas, and the BCM Center for Skeletal Medicine and Biology and the Pamela and David Ott Center for Heritable Disorders of Connective Tissue, and PMR Foundation: ERF Matterson Grant

REFERENCES

1. Nourissat G, Berenbaum F, Duprez D. Tendon injury: from biology to tendon repair. Nat Rev Rheumatol 2015; 11: 223-233.
2. Screen HR, Berk DE, Kadler KE, Ramirez F, Young MF. Tendon functional extracellular matrix. J Orthop Res 2015; 33: 793-799.
3. Kannus P. Structure of the tendon connective tissue. Scand J Med Sci Sports 2000; 10: 312-320.
4. Kalson NS, Lu Y, Taylor SH, Starborg T, Holmes DF, Kadler KE. A structure-based extracellular matrix expansion mechanism of fibrous tissue growth. Elife 2015; 4.
5. Saito M, Marumo K. Collagen cross-links as a determinant of bone quality: a possible explanation for bone fragility in aging, osteoporosis, and diabetes mellitus. Osteoporos Int 2010; 21: 195-214.
6. Alford AI, Kozloff KM, Hankenson KD. Extracellular matrix networks in bone remodeling. Int J Biochem Cell Biol 2015; 65: 20-31.
7. Lim J, Grafe I, Alexander S, Lee B. Genetic causes and mechanisms of Osteogenesis Imperfecta. Bone 2017; 102: 40-49.
8. Arponen H, Makitie O, Waltimo-Siren J. Association between joint hypermobility, scoliosis, and cranial base anomalies in paediatric Osteogenesis imperfecta patients: a retrospective cross-sectional study. BMC Musculoskelet Disord 2014; 15: 428.
9. Primorac D, Anticevic D, Barisic I, Hudetz D, Ivkovic A. Osteogenesis imperfecta--multi-systemic and life-long disease that affects whole family. Coll Antropol 2014; 38: 767-772.
10. Hudson DM, Eyre DR. Collagen prolyl 3-hydroxylation: a major role for a minor post-translational modification? Connect Tissue Res 2013; 54: 245-251.

438 11. Morello R, Bertin TK, Chen Y, Hicks J, Tonachini L, Monticone M, et al. CRTAP is
439 required for prolyl 3- hydroxylation and mutations cause recessive osteogenesis imperfecta.
440 Cell 2006; 127: 291-304.
441 12. Baldridge D, Schwarze U, Morello R, Lennington J, Bertin TK, Pace JM, et al. CRTAP and
442 LEPRE1 mutations in recessive osteogenesis imperfecta. Hum Mutat 2008; 29: 1435-1442.
443 13. Barnes AM, Chang W, Morello R, Cabral WA, Weis M, Eyre DR, et al. Deficiency of
444 cartilage-associated protein in recessive lethal osteogenesis imperfecta. N Engl J Med 2006;
445 355: 2757-2764.
446 14. Cabral WA, Chang W, Barnes AM, Weis M, Scott MA, Leikin S, et al. Prolyl 3-hydroxylase
447 1 deficiency causes a recessive metabolic bone disorder resembling lethal/severe
448 osteogenesis imperfecta. Nat Genet 2007; 39: 359-365.
449 15. van Dijk FS, Nesbitt IM, Zwikstra EH, Nikkels PG, Piersma SR, Fratantoni SA, et al. PPIB
450 mutations cause severe osteogenesis imperfecta. Am J Hum Genet 2009; 85: 521-527.
451 16. Baldridge D, Lennington J, Weis M, Homan EP, Jiang MM, Munivez E, et al. Generalized
452 connective tissue disease in *Crtap*$^{-/-}$ mouse. PLoS One 2010; 5: e10560.
453 17. Chen F, Guo R, Itoh S, Moreno L, Rosenthal E, Zappitelli T, et al. First mouse model for
454 combined osteogenesis imperfecta and Ehlers-Danlos syndrome. J Bone Miner Res 2014; 29:
455 1412-1423.
456 18. Terajima M, Taga Y, Chen Y, Cabral WA, Hou-Fu G, Srisawasdi S, et al. Cyclophilin-B
457 modulates collagen cross-linking by differentially affecting lysine hydroxylation in the
458 helical and telopeptidyl domains of tendon type I collagen. J Biol Chem 2016; 291: 9501-
459 9512.

19. Vranka JA, Pokidysheva E, Hayashi L, Zientek K, Mizuno K, Ishikawa Y, et al. Prolyl 3-hydroxylase 1 null mice display abnormalities in fibrillar collagen-rich tissues such as tendons, skin, and bones. J Biol Chem 2010; 285: 17253-17262.
20. Nixon AJ, Grol MW, Lang HM, Ruan MZC, Stone A, Begum L, et al. Disease-modifying osteoarthritis treatment with interleukin-1 receptor antagonist gene therapy in small and large animal models. Arthritis Rheumatol 2018; 70: 1757-1768.
21. Ruan MZ, Dawson B, Jiang MM, Gannon F, Heggeness M, Lee BH. Quantitative imaging of murine osteoarthritic cartilage by phase-contrast micro-computed tomography. Arthritis Rheum 2013; 65: 388-396.
22. Ruan MZ, Erez A, Guse K, Dawson B, Bertin T, Chen Y, et al. Proteoglycan 4 expression protects against the development of osteoarthritis. Sci Transl Med 2013; 5: 176ra134.
23. Stone A, Grol MW, Ruan MZC, Dawson B, Chen Y, Jiang MM, et al. Combinatorial *Prg4* and *Il-1ra* gene therapy protects against hyperalgesia and cartilage degeneration in post-traumatic osteoarthritis. Hum Gene Ther 2019; 30: 225-235.
24. Schindelin J, Arganda-Carreras I, Frise E, Kaynig V, Longair M, Pietzsch T, et al. Fiji: an open-source platform for biological-image analysis. Nat Methods 2012; 9: 676-682.
25. Eyre D. Collagen cross-linking amino acids. Methods Enzymol 1987; 144: 115-139.
26. Hudson DM, Archer M, King KB, Eyre DR. Glycation of type I collagen selectively targets the same helical domain lysine sites as lysyl oxidase-mediated cross-linking. J Biol Chem 2018; 293: 15620-15627.
27. Steinmann S, Pfeifer CG, Brochhausen C, Docheva D. Spectrum of tendon pathologies: triggers, trails and end-state. Int J Mol Sci 2020; 21.

28. Grafe I, Yang T, Alexander S, Homan EP, Lietman C, Jiang MM, et al. Excessive transforming growth factor-beta signaling is a common mechanism in osteogenesis imperfecta. Nat Med 2014; 20: 670-675.

29. Lim J, Munivez E, Jiang MM, Song IW, Gannon F, Keene DR, et al. mTORC1 signaling is a critical regulator of postnatal tendon development. Sci Rep 2017; 7: 17175.

30. Bateman JF, Boot-Handford RP, Lamande SR. Genetic diseases of connective tissues: cellular and extracellular effects of ECM mutations. Nat Rev Genet 2009; 10: 173-183.

31. Taga Y, Kusubata M, Ogawa-Goto K, Hattori S. Developmental stage-dependent regulation of prolyl 3-hydroxylation in tendon type I collagen. J Biol Chem 2016; 291: 837-847.

32. Garman CR, Graf A, Krzak J, Caudill A, Smith P, Harris G. Gait deviations in children with Osteogenesis Imperfecta Type I. J Pediatr Orthop 2019; 39: e641-e646.

33. Abdelaziz DM, Abdullah S, Magnussen C, Ribeiro-da-Silva A, Komarova SV, Rauch F, et al. Behavioral signs of pain and functional impairment in a mouse model of osteogenesis imperfecta. Bone 2015; 81: 400-406.

FIGURE LEGENDS

Figure 1. **Loss of Crtap causes thinning and hypercellularity of tendons and ligaments in young and mature mice.** A-C, representative H&E images of 1-month ankle joints. D-F, representative H&E images of 1-month knee joints. G-I, representative H&E images of 4-month ankle joints. J-L, representative H&E images of 4-month knee joints. For all micrographs, higher magnification images of the myotendinous junction (bottom-left), mid-tendon (bottom-center) and insertion (bottom-right) are illustrated. n = 3-4 mice per group. Scale bar is 1 mm. M, representative phase-contrast μCT images of 4-month wildtype (left) and *Crtap*$^{-/-}$ (right) knee joints. Blue indicates the patellar ligament, green indicates the femoral articular cartilage, and red indicates the tibial articular cartilage. Scale bar is 1 mm. N, volumetric quantification of the patellar ligament volume in wildtype, heterozygous and *Crtap*$^{-/-}$ mice. * indicates $p < 0.05$. n = 3 mice per group.

Figure 2. **Collagen fibril diameter is altered in tendons and ligaments from heterozygous and *Crtap*$^{-/-}$ mice.** A-C, representative TEM images of 4-month FDL tendon collagen fibrils. Scale bar is 500 nm. D, representative histogram of size distribution for collagen fibrils in FDL tendons. Data are representative of n = 3 mice. E-G, representative TEM images of 4-month Achilles tendon collagen fibrils. Scale bar is 500 nm. H, representative histogram of size distribution for collagen fibrils in Achilles tendons. Data are representative of n = 3 mice. E-G, representative TEM images of 4-month patellar ligament collagen fibrils. Scale bar is 500 nm. H, representative histogram of size distribution for collagen fibrils in patellar ligaments. Data are representative of n = 3 mice per group.

Figure 3. **Collagen cross-linking is increased in tendons and ligaments from young and mature *Crtap*$^{-/-}$ mice.** Quantification of collagen cross-links as hydroxylysyl-pyridinoline (HP) residues per collagen for: A, FDL tendons; B, Achilles tendons; and C, patellar ligaments. Data are means ± S.D. * indicates $p < 0.05$. n = 3-4 mice per group.

Figure 4. **Motor activity and coordination is impaired in 4-month-old *Crtap*$^{-/-}$ mice.** A-B, quantification of spontaneous motor activity including (A) horizontal and (B) vertical activity over a 30-min period using the open field assay. Data are min-to-max box and whisker plots with individual points indicated. C, quantification of motor activity, coordination and endurance across 10 trials conducted over 2 days using an accelerating rotarod assay. Data are means ± S.D. Black asterisks indicates $p < 0.05$ compared to wildtype mice, and blue asterisks indicates $p < 0.05$ compared to heterozygous mice. D-E, quantification of (D) forelimb and (E) hindlimb motor coordination using the grid footslip assay. Data are min-to-max box and whisker plots with individual points indicated. F, quantification of forelimb and hindlimb grip strength using the inverted grid assay conducted for 120 s. A reduction in the latency to fall indicates a reduced grip strength. Data are min-to-max box and whisker plots with individual points indicated. G, quantification of forelimb grip strength in N of force measured over 3 trials and then averaged. Data are min-to-max box and whisker plots with individual points indicated. For all experiments, * indicates $p < 0.05$. n = 9-12 mice per group.

FIGURE 1

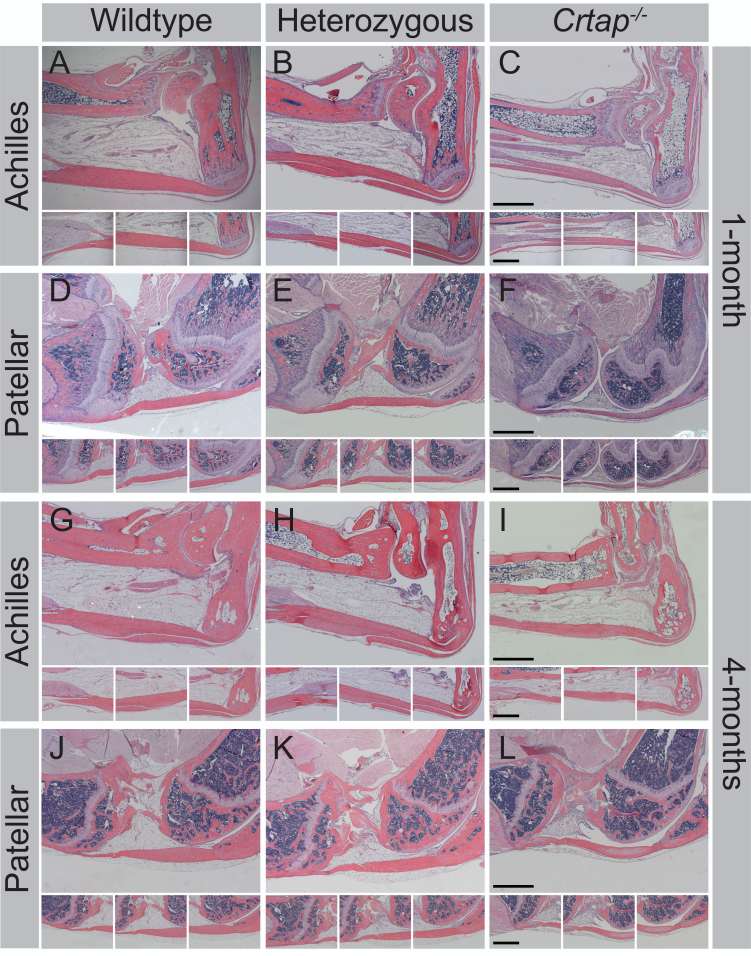
Wildtype
Heterozygous
Crtap-/-
A
B
C
Achilles
1-month
D
E
F
Patellar
G
H
I
Achilles
4-months
J
K
L
Patellar

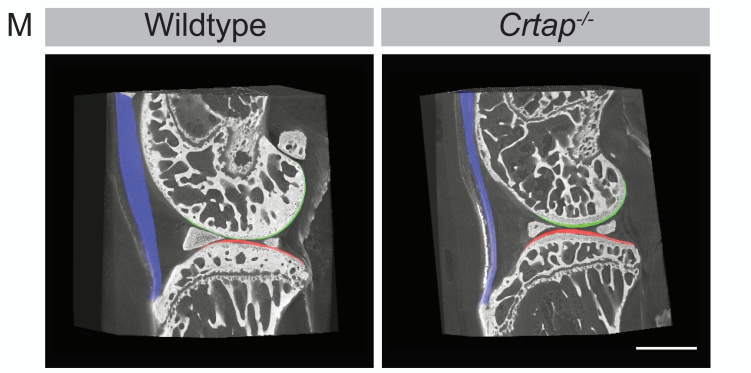
M
Wildtype
Crtap-/-

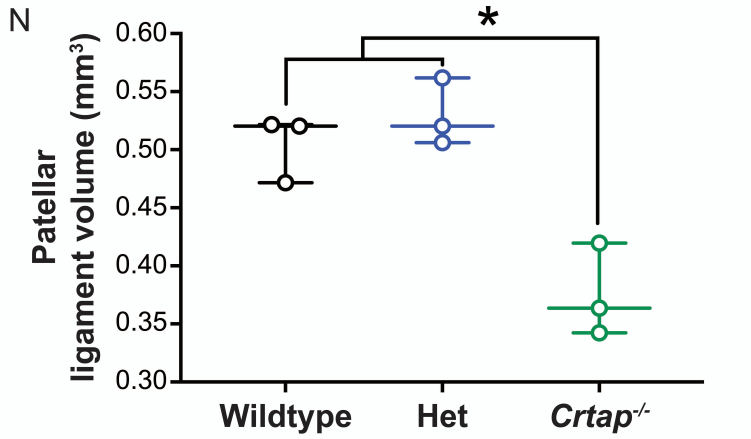
N
Patellar ligament volume (mm3)
0.60
0.55
0.50
0.45
0.40
0.35
0.30
*
Wildtype
Het
Crtap-/-

FIGURE 2

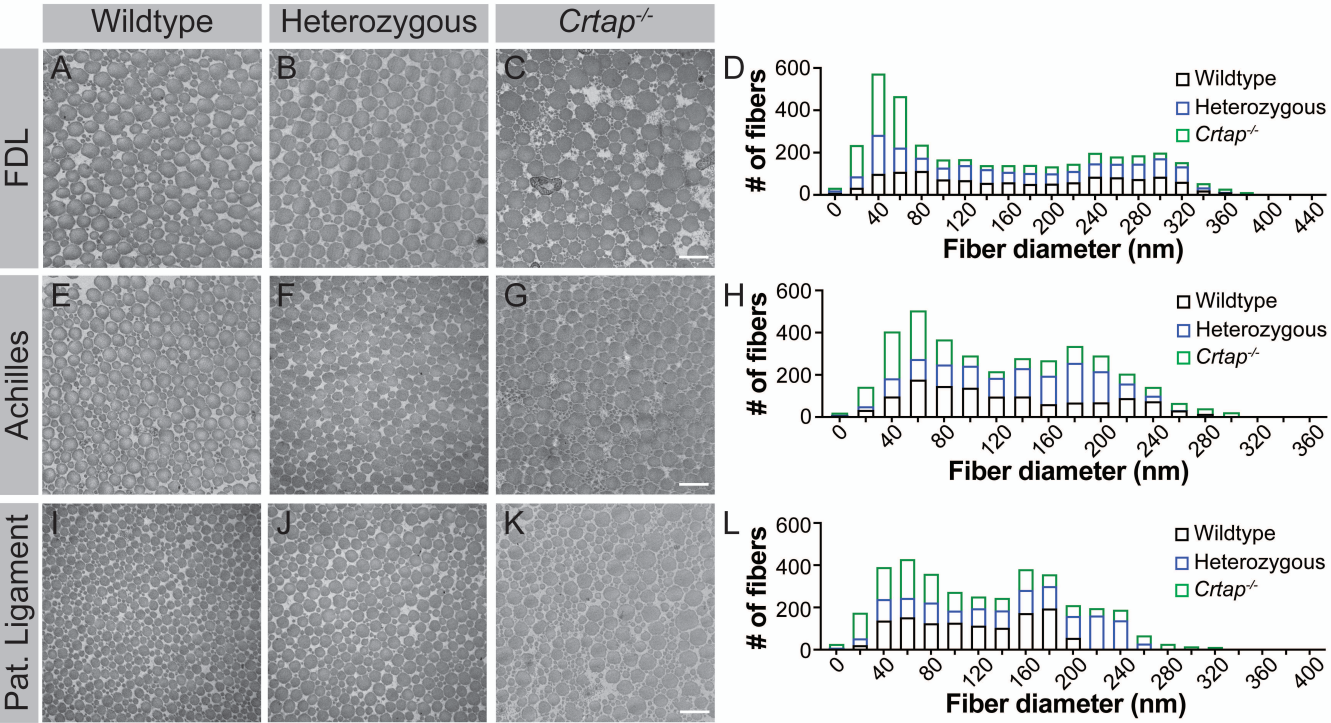
Wildtype
Heterozygous
Crtap-/-
FDL
Achilles
Pat. Ligament
A
B
C
D
E
F
G
H
I
J
K
L
# of fibers
Fiber diameter (nm)
Wildtype
Heterozygous
Crtap-/-
0
40
80
120
160
200
240
280
320
360
400
440
600

FIGURE 3

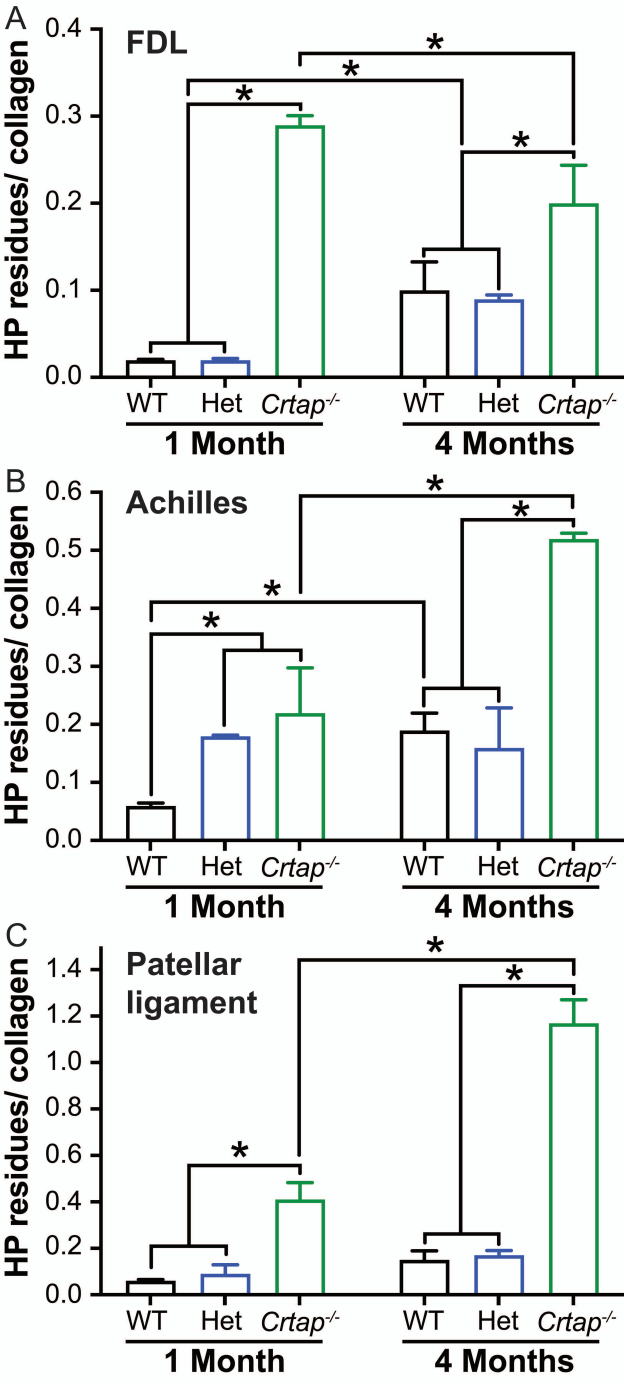
A
FDL
HP residues/ collagen
0.4
0.3
0.2
0.1
0.0
*
*
*
WT
Het
Crtap-/-
WT
Het
Crtap-/-
1 Month
4 Months
B
Achilles
HP residues/ collagen
0.6
0.5
0.4
0.3
0.2
0.1
0.0
*
*
*
WT
Het
Crtap-/-
WT
Het
Crtap-/-
1 Month
4 Months
C
Patellar ligament
HP residues/ collagen
1.4
1.2
1.0
0.8
0.6
0.4
0.2
0.0
*
*
*
WT
Het
Crtap-/-
WT
Het
Crtap-/-
1 Month
4 Months

FIGURE 4

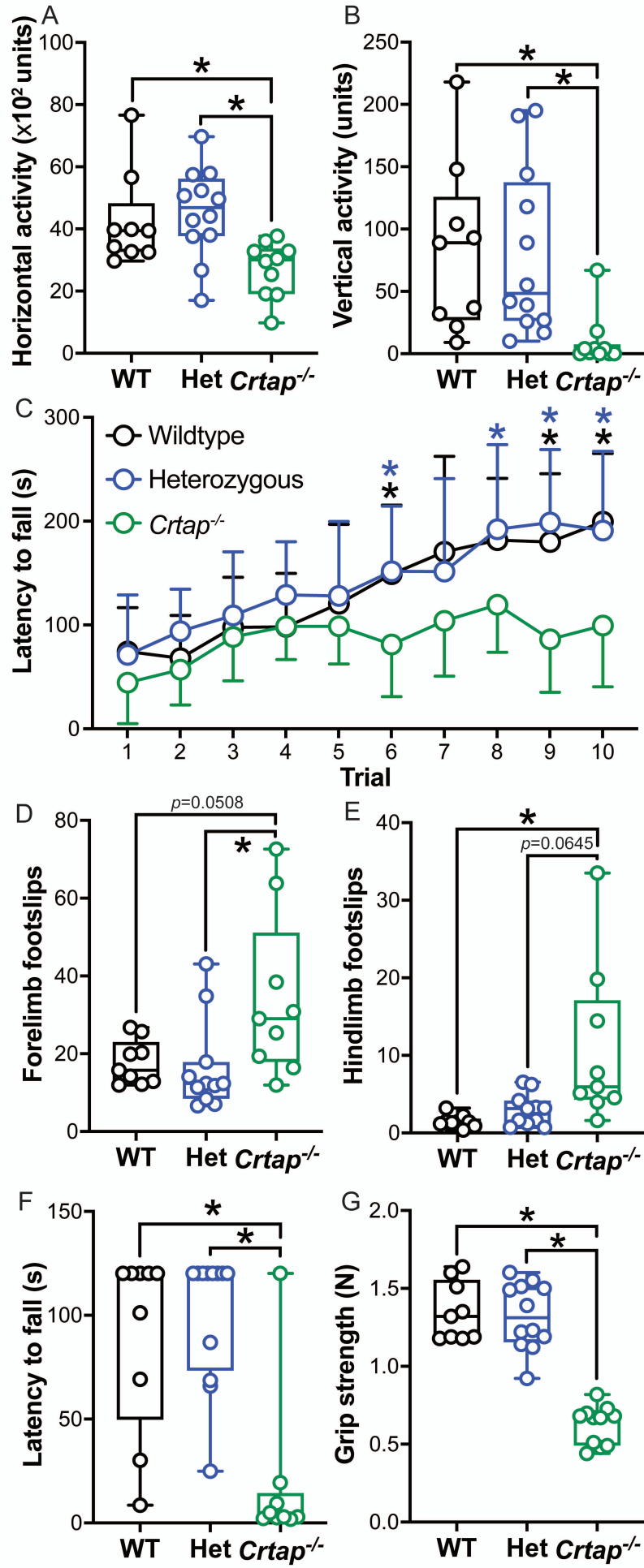
A
Horizontal activity (x10² units)
100
80
60
40
20
0
*
*
WT
Het Crtap-/-
B
Vertical activity (units)
250
200
150
100
50
0
*
*
WT
Het Crtap-/-
C
Latency to fall (s)
300
200
100
0
Wildtype
Heterozygous
Crtap-/-
* * * * *
1 2 3 4 5 6 7 8 9 10
Trial
D
Forelimb footslips
80
60
40
20
0
p=0.0508
*
WT
Het Crtap-/-
E
Hindlimb footslips
40
30
20
10
0
*
p=0.0645
WT
Het Crtap-/-
F
Latency to fall (s)
150
100
50
0
*
*
WT
Het Crtap-/-
G
Grip strength (N)
2.0
1.5
1.0
0.5
0.0
*
*
WT
Het Crtap-/-